Development 139, 749-759 (2012) doi:10.1242/dev.074138

Jmjd5, an H3K36me2 histone demethylase, modulates embryonic cell proliferation through the regulation of *Cdkn1a* expression

Akihiko Ishimura[1], Ken-ichi Minehata[2], Minoru Terashima[1], Gen Kondoh[3], Takahiko Hara[2] and Takeshi Suzuki[1,*]

SUMMARY

Covalent modifications of histones play an important role in chromatin architecture and dynamics. In particular, histone lysine methylation is important for transcriptional control during diverse biological processes. The nuclear protein Jmjd5 (also called Kdm8) is a histone lysine demethylase that contains a JmjC domain in the C-terminal region. In this study, we have generated *Jmjd5*-deficient mice (*Jmjd5*$^{\Delta/\Delta}$) to investigate the in vivo function of *Jmjd5*. *Jmjd5*$^{\Delta/\Delta}$ embryos showed severe growth retardation, resulting in embryonic lethality at the mid-gestation stage. Mouse embryonic fibroblasts (MEFs) derived from *Jmjd5* hypomorphic embryos (*Jmjd5*$^{neo/neo}$) also showed the growth defect. Quantitative PCR analysis of various cell cycle regulators indicated that only *Cdkn1a* expression was upregulated in *Jmjd5*$^{neo/neo}$ MEFs and *Jmjd5*$^{\Delta/\Delta}$ embryos. A knockdown assay with *Cdkn1a*-specific small interfering RNAs revealed that the growth defect of *Jmjd5*$^{neo/neo}$ MEFs was significantly rescued. In addition, a genetic study using *Jmjd5*$^{\Delta/\Delta}$; *Cdkn1a*$^{\Delta/\Delta}$ double-knockout mice showed that the growth retardation of *Jmjd5*$^{\Delta/\Delta}$ embryos was partially rescued by *Cdkn1a* deficiency. Chromatin immunoprecipitation analysis showed that increased di-methylated lysine 36 of histone H3 (H3K36me2) and reduced recruitment of endogenous Jmjd5 were detected in the transcribed regions of *Cdkn1a* in *Jmjd5*$^{neo/neo}$ MEFs. Taken together, these results suggest that Jmjd5 physiologically moderates embryonic cell proliferation through the epigenetic control of *Cdkn1a* expression.

KEY WORDS: Jmjd5 (Kdm8), Cdkn1a, Cell proliferation, Mouse

INTRODUCTION

In eukaryotic nuclei, genomic DNA is efficiently packaged into chromatin, which is made up of numerous nucleosomes. In each nucleosome, ~146 bp of DNA is wrapped around a histone octamer comprising two copies of four core histones: H2A, H2B, H3 and H4. Histone H1, the linker histone, helps to further compact the nucleosomal DNA into higher-order structures. In addition, the flexible N-termini that extend from the core histones (the histone tails) post-translationally receive various covalent modifications such as methylation, acetylation, phosphorylation, ubiquitylation and sumoylation. These histone modifications can alter the structure of the nucleosome and may also affect the assembly between chromatin and the nuclear proteins that recognize specific histone modifications (Mosammaparast and Shi, 2011).

Among these modifications, methylation of specific lysine residues on histone H3 (e.g. H3K4, H3K9, H3K27 and H3K36) is closely related to gene expression (Martin and Zhang, 2005). During transcriptional processes, methylation at H3K4 and H3K36 correlates with transcriptionally active genes, whereas methylation at H3K9 and H3K27 is linked to transcriptional repression. To add more complexity, each of the lysine residues has four distinct methylation states: un-, mono- (me1), di- (me2) or tri- (me3) methylated. Importantly, methylation is a reversible modification regulated by histone lysine methyltransferases (KMTs) or histone lysine demethylases (KDMs). The methylation status of histone H3 is dynamically regulated by KMTs and KDMs and is implicated in diverse biological processes including cellular proliferation, differentiation, DNA repair and recombination.

Two classes of KDMs have been identified (Klose et al., 2006). KDM1 (also called LSD1) encodes a flavin adenine dinucleotide-dependent amine oxidase and is known to remove mono- and di-methylated lysine modifications. The Jumonji C (JmjC) domain family of KDMs contains proteins that are Fe(II)- and α-ketoglutarate-dependent enzymes. Unlike KDM1, JmjC proteins can remove all three methylation states. Recent studies suggest that the dysregulation of JmjC members is associated with human diseases such as neurological disorders and cancers (Pedersen and Helin, 2010). For instance, mutations in *KDM5C* (*JARID1C*) were found in patients with X-linked mental retardation (XLMR) (Jensen et al., 2005), and *PHF8* mutations were also observed in patients with XLMR and cleft lip/palate (Abidi et al., 2007; Koivisto et al., 2007; Laumonnier et al., 2005). Gene amplification of *KDM4A* (*JMJD2C*) was detected in esophageal squamous carcinomas, medulloblastoma and breast cancer (Ehrbrecht et al., 2006; Liu et al., 2009; Northcott et al., 2009; Yang et al., 2000), and elevated expression of *KDM5B* (*PLU1*) has been reported in breast, prostate and lung cancers (Hayami et al., 2010; Lu et al., 1999; Xiang et al., 2007). Furthermore, inactivating somatic mutations of *KDM6A* (*UTX*) have been reported in multiple tumor types (van Haaften et al., 2009).

Studies of mice genetically modified for several JmjC members suggest the involvement of JmjC proteins in various pathological/developmental processes. For example, deletion of

[1]Division of Functional Genomics, Cancer Research Institute, Kanazawa University, Kakuma-machi, Kanazawa, Ishikawa 920-1192, Japan. [2]Stem Cell Project Group, Tokyo Metropolitan Institute of Medical Science, 2-1-6 Kamikitazawa, Setagaya-ku, Tokyo 156-8506, Japan. [3]Laboratory of Animal Experiments for Regeneration, Institute for Frontier Medical Science, Kyoto University, Shogoin-kawahara-cho 53, Sakyo-ku, Kyoto 606-8507, Japan.

*Author for correspondence (suzuki-t@staff.kanazawa-u.ac.jp)

Accepted 16 December 2011

Kdm3a (*Jmjd1a*) showed an adult-onset obesity phenotype and the downregulation of several metabolic genes (Inagaki et al., 2009; Tateishi et al., 2009). Deletion of *Kdm2b* (*Fbxl10*) showed an exencephalic phenotype and caused increased cell proliferation and cell death in neural progenitor cells, indicating an essential role for this gene during neural development (Fukuda et al., 2011).

Recently, JMJD5 (KDM8), a member of the JmjC family, was reported to be a demethylase for di-methylated lysine 36 of histone H3 (H3K36me2), regulating the expression of the *CCNA1* gene in MCF7 breast cancer cells (Hsia et al., 2010). In *Arabidopsis thaliana*, Jmjd5 was reported to be co-regulated with evening-phased clock components and to be positively associated with clock genes expressed at dawn (Jones et al., 2010). These authors also showed that knockdown of *JMJD5* in U2OS osteosarcoma cells led to fast-running circadian oscillations, suggesting its interchangeable role in both plant and human circadian systems. However, the physiological role of *Jmjd5* in the context of a whole mammalian organism remains unknown.

In order to understand the function of *Jmjd5* in cellular and developmental processes, we generated *Jmjd5* mutant mice. Deletion of the *Jmjd5* allele caused severe growth retardation, resulting in embryonic lethality at mid-gestation. Mouse embryonic fibroblasts (MEFs) derived from *Jmjd5* hypomorphic embryos also showed the defect in cell proliferation. We identified increased expression of *Cdkn1a* as one of the mechanisms leading to cell growth retardation. ChIP analysis indicated that Jmjd5 is directly recruited to the *Cdkn1a* locus, resulting in the alteration of the H3K36me2 status of *Cdkn1a*. These results suggest that the Jmjd5 histone demethylase is involved in embryonic cell proliferation by fine-tuning the expression of *Cdkn1a*.

MATERIALS AND METHODS

Generation of *Jmjd5*-deficient mice

The targeting vector for *Jmjd5*-deficient mice was constructed using a recombineering system (Liu et al., 2003). The vector was first linearized by *Pme*I digestion and used for electroporation into the V6.5 clone derived from C57BL/6 and 129Sv embryonic stem (ES) cells (Eggan et al., 2001). The cells were subjected to G418 selection (150 μg/ml) and independent colonies were screened by Southern blotting. Genomic DNAs isolated from ES cell clones were digested with *Cla*I or *Eco*RV and hybridized with a 5′ probe (nucleotides 4641 to 5187 in NCBI reference sequence NC_000073.5) or a 3′ probe (nucleotides 13709 to 14028), respectively. These probes were generated by PCR using the following primers: for 5′ probe, 5′-TCCCTTACACGGCTATGGTC-3′ and 5′-AGCTGAGAG-AATTCAGGGCA-3′; for 3′ probe, 5′-GGGTGAGTCAGAATAGTGTA-3′ and 5′-TCATTGGCCAAGGATTCAGA-3′.

One derivative of each ES cell line containing the floxed *Jmjd5* allele was injected into the blastocoel cavity of E3.5 C57BL/6 blastocysts. Chimeric mice were generated at UNITECH (Japan) and mated with C57BL/6 females. The offspring ($Jmjd5^{+/neo}$) were screened for germline transmission by PCR. F1 mice were backcrossed with C57BL/6 mice. *CAG-Flp* transgenic mice (Kanki et al., 2006), *Pgk2-Cre* transgenic mice (Ando et al., 2000) and *Cdkn1a*-deficient mice (Deng et al., 1995) were used for the generation of $Jmjd5^{flox/flox}$ mice, $Jmjd5^{\Delta/\Delta}$ mice and $Jmjd5^{\Delta/\Delta}$; $Cdkn1a^{\Delta/\Delta}$ mice, respectively. All animal experiments were approved by the Animal Care and Use Committee of Kanazawa University.

Genotyping of *Jmjd5*-deficient mice

For genotyping adult mice, tail tissue was lysed in lysis buffer (20 mM Tris-HCl pH 8.0, 5 mM EDTA, 400 mM NaCl, 0.3% SDS, 0.2 mg/ml proteinase K) for DNA extraction. Genomic DNA was used for PCR using Ex-Taq DNA polymerase (Takara) or Southern blotting. For genotyping embryos, a part of the yolk sac was lysed and the lysate was used for direct PCR using MightyAmp DNA polymerase (Takara). The primers used for genotyping are listed in supplementary material Table S1. For Southern blotting, genomic DNA was digested with *Stu*I or *Kpn*I and hybridized with a *Jmjd5*-specific probe (nucleotides 10833 to 11233 in NCBI reference sequence NC_000073.5). Signals were visualized with the Gene Image Random-Prime Labeling and Detection System (Amersham). The probe was amplified using primers 5′-TTCTGACCTCCACATATGACACAG-3′ and 5′-CCAACCTGACTCAACCTACTCC-3′.

Preparation of *Jmjd5* hypomorphic MEFs

MEFs were established from wild-type and $Jmjd5^{neo/neo}$ embryos using standard protocols (Nagy et al., 2003) and cultured in Dulbecco's modified Eagle's medium (DMEM) with 10% fetal bovine serum, 2 mM glutamine and penicillin/streptomycin at 37°C in 5% CO_2. For the cell growth assay, 3×10^4 cells were plated on 12-well plates and the cell number was counted every 24 hours. For retroviral infection, 1.5×10^5 cells were plated on 6-well plates and the cell number was counted 48 hours after infection.

Preparation of plasmids and anti-Jmjd5 antibody

For whole-mount in situ hybridization, a fragment of *Jmjd5* cDNA (nucleotides 73 to 1502 in NCBI reference sequence NM_029842.5) or *Cdkn1a* cDNA (nucleotides 104 to 587 in NCBI reference sequence NM_007669.4) was amplified and cloned into the pSTBlue-1 vector (Novagen). For the luciferase assay, pTAL-Luc (Clontech) was used as a control vector (tk-luc). To prepare p53-responsive luciferase vector (p53BS), the complementary oligonucleotides 5′-GAGAACATGTCCCAACATGTTG-3′ and 5′-TCCAACATGTT-GGGACATGTTC-3′, which correspond to the p53 binding site from the human *CDKN1A* locus (El-Deiry et al., 1993), were synthesized. Six annealed oligonucleotides were tandemly ligated and inserted into pTAL-Luc.

Mouse *Jmjd5* cDNA was tagged with FLAG-His_6 tag and cloned into the pDON-5 Neo plasmid (Takara) to produce retroviruses. A Jmjd5 H319A mutant, which corresponds to the catalytically inactive JMJD5 mutant H321A in humans (Hsia et al., 2010), was generated using a PCR-based mutagenesis kit (Takara). The shRNA-expressing retroviruses were constructed and produced as described previously (Yoshida et al., 2011). Oligonucleotides for shRNA production are listed in supplementary material Table S2.

For the preparation of anti-Jmjd5 rabbit polyclonal antibody, histidine-tagged C-terminal Jmjd5 (D175 to Y396) proteins purified from genetically engineered *Escherichia coli* were used.

Quantitative reverse transcription PCR (qRT-PCR)

Total RNA was extracted with Trizol (Invitrogen) and cDNA prepared using the SuperScript VILO cDNA Synthesis Kit (Invitrogen). qRT-PCR analysis was performed with FastStart Universal SYBR Green Master (Roche) using the 7900HT Fast Real-Time PCR System (Applied Biosystems). PCR data were normalized to the expression of *Gapdh*. qPCR primers are listed in supplementary material Table S1.

Chromatin immunoprecipitation (ChIP) analysis

ChIP experiments were performed as described previously (Kimura et al., 2008). The complexes that were immunoprecipitated with anti-K36me2 mouse monoclonal antibody or anti-Jmjd5 antibody were collected using Dynabeads coupled with protein A or G (Invitrogen). The precipitates were used for the detection of *Cdkn1a* genomic regions by qPCR. ChIP primers are listed in supplementary material Table S1.

Knockdown assay

Each Stealth RNAi for *Cdkn1a* (Invitrogen) was introduced into cells using Lipofectamine RNAiMAX (Invitrogen) by a reverse transfection procedure. The cells were collected for RNA extraction after 48 hours, or the cell number was counted after 72 hours. The Stealth RNAi Negative Control Kit (Invitrogen) was used for control. The siRNAs used for this study are listed in supplementary material Table S2.

Immunoblotting

MEFs were lysed in RIPA buffer [50 mM Tris-HCl pH 7.5, 150 mM NaCl, 1% NP40, 0.1% SDS, 1 mM EDTA supplemented with 500 μM 4-(2-aminoethyl)benzenesulfonyl fluoride hydrochloride, 150 nM

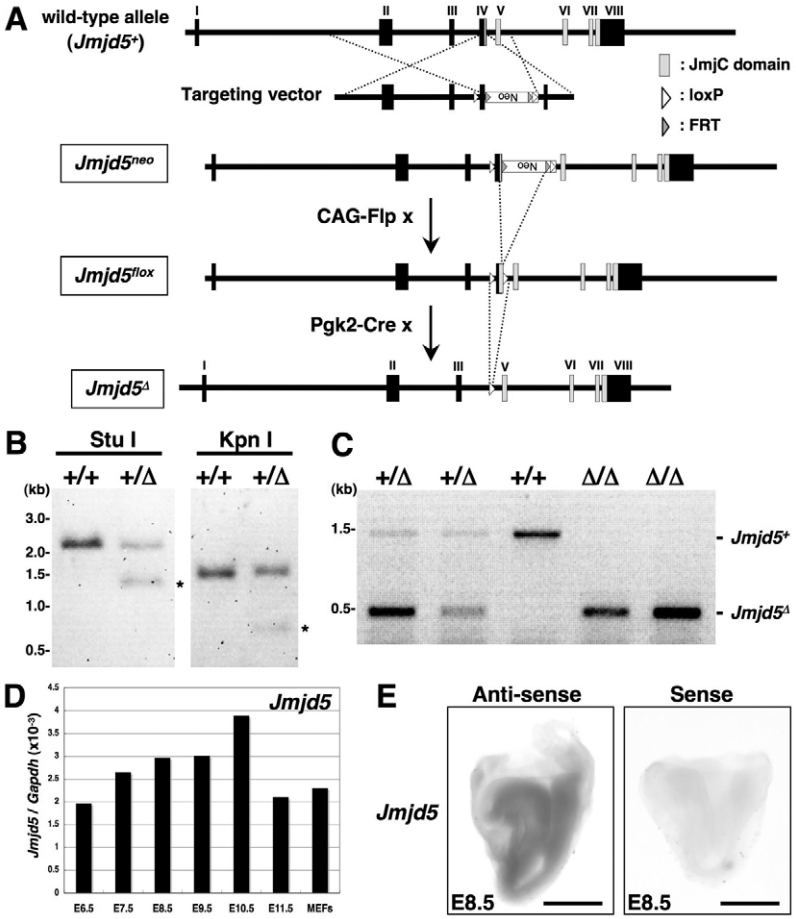

Fig. 1. Generation of *Jmjd5*-deficient mice and the expression of *Jmjd5* during early embryogenesis. (**A**) Exon-intron structure of the *Jmjd5* allele (*Jmjd5*$^{+}$) and targeting strategy to generate *Jmjd5*-deficient mice. The *Jmjd5*$^{+}$ allele contains eight exons (black boxes), and exon IV contains the 5′ region of the JmjC domain (light-gray boxes). The targeting vector contains the *Pgk-Neo* cassette (white box), a pair of *loxP* sequences (white arrowheads) and FRT sequences (gray arrowheads). In the *Jmjd5*^{neo} allele, the targeting vector is inserted in the *Jmjd5*$^{+}$ allele. The *Pgk-Neo* cassette is removed by mating with *CAG-Flp* mice to generate the *Jmjd5*^{flox} allele. *Jmjd5*$^{flox/flox}$ mice are mated with *Pgk2-Cre* mice to establish mutant mice with the *Jmjd5* deletion (*Jmjd5*$^{\Delta}$). (**B**) Southern blotting of tail DNA to distinguish wild-type and *Jmjd5*$^{+/\Delta}$ mice (see text). (**C**) Genotyping PCR using genomic DNA from E10.5 littermates of *Jmjd5*$^{+/\Delta}$ intercrosses. (**D**) qRT-PCR analysis of endogenous *Jmjd5* expression during embryogenesis using *Jmjd5*-specific primers. (**E**) WISH analysis of an E8.5 embryo with the sense or the complementary antisense probe for *Jmjd5*. Scale bars: 400 μm.

aprotinin, 1 μM E-64 and 1 μM leupeptin]. The lysates were separated on a SuperSep Ace 5-20% running gel (Wako). Anti-p21 (SX118, BD Biosciences), anti-p53 (FL393, Santa Cruz) and anti-Gapdh (6C5, Millipore) antibodies were used. As a positive control for the detection of endogenous p21 and p53, wild-type MEFs were treated with 0.03 μg/ml adriamycin for 24 hours.

Senescence-associated β-galactosidase (SA-β-gal) staining and immunofluorescence

SA-β-gal staining was performed as described (Kitajima et al., 2011). As a positive control for the detection of senescent cells, MEFs (1×10^4 cells) were sparsely seeded on 6-well plates and cultured for 15 days. For immunofluorescence, MEFs were fixed with 4% paraformaldehyde in phosphate-buffered saline. The specimens were incubated with anti-single-stranded DNA (ssDNA) antibody (Dako) and treated with Alexa 546-conjugated anti-rabbit IgG antibody (Invitrogen). Nuclei were visualized with 4′,6-diamidino-2-phenylindole (DAPI). As a positive control for the detection of apoptotic cells, wild-type MEFs were treated with 0.06 μg/ml adriamycin for 24 hours.

Whole-mount in situ hybridization (WISH) analysis

WISH of mouse embryos was performed as described previously (Yamaguchi et al., 1993) with the exception that hybridization was performed at 70°C. Digoxygenin (DIG)-labeled RNA probes were synthesized using the DIG RNA Labeling Mix (Roche).

Luciferase assay

Reporter vector was introduced into wild-type MEFs or *Jmjd5*$^{neo/neo}$ MEFs using the Fugene HD Transfection Reagent (Roche). The cells were collected after 48 hours and the luciferase activities determined using the Dual-Luciferase Reporter Assay System (Promega).

RESULTS

Jmjd5-deficient mice exhibit embryonic lethality at mid-gestation

In order to investigate the in vivo function of *Jmjd5*, we generated conditional *Jmjd5* knockout mice (*Jmjd5*$^{flox/flox}$) by the targeted disruption of exon IV, which encodes the start of the JmjC domain (Fig. 1A). Recombination of the *Jmjd5*^{flox} allele by Cre recombinase causes a frame-shift mutation, resulting in the lack of production for Jmjd5 protein with a JmjC domain. We mated *Jmjd5*$^{flox/flox}$ female mice with spermatocyte-specific Cre-expressing transgenic male mice (*Pgk2-Cre*) (Ando et al., 2000), and mutant mice with a *Jmjd5* deletion allele (*Jmjd5*$^{\Delta}$) were established. *Jmjd5*$^{+/\Delta}$ heterozygous mice were viable and fertile, and no morphological changes were observed as compared with wild-type mice. To generate *Jmjd5* null mice (*Jmjd5*$^{\Delta/\Delta}$), *Jmjd5*$^{+/\Delta}$ mice were intercrossed, and the genotype for each mouse was determined by Southern blot analysis with a *Jmjd5*-specific probe. As shown in Fig. 1B, this probe was able to recognize the 2.3 kb wild-type and 1.4 kb mutant fragments from *Stu*I-digested genomic DNA as well as the 1.6 kb wild-type and 0.7 kb mutant fragments from *Kpn*I-digested genomic DNA. However, we could not find *Jmjd5*$^{\Delta/\Delta}$ homozygous mice among the offspring (supplementary material Table S3), suggesting that the *Jmjd5*$^{\Delta/\Delta}$ genotype was embryonic lethal. Thus, we performed further genotyping analyses at various embryonic stages. The genotype for each embryo was determined by PCR analysis, which was able to detect a 1.5 kb band for the wild-type allele and a 0.5 kb band for the mutant allele (Fig. 1C).

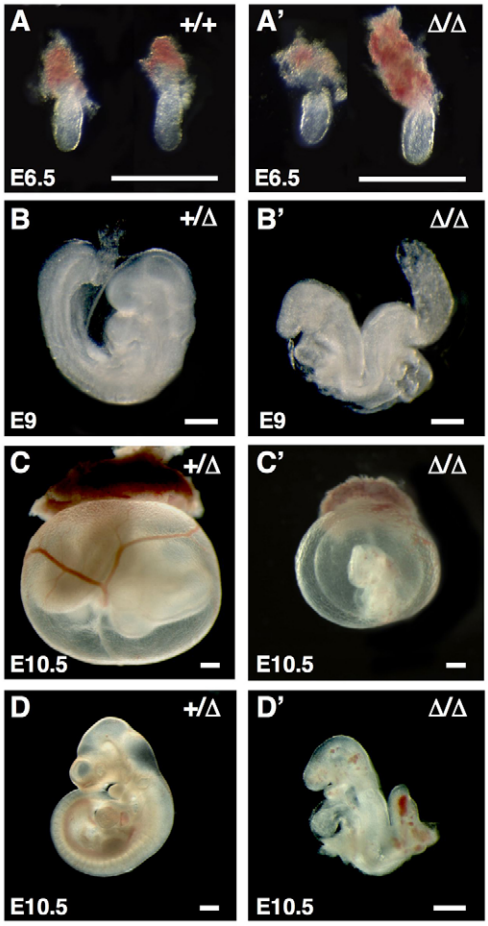

Fig. 2. Phenotype of *Jmjd5*$^{\Delta/\Delta}$ embryos. Phenotypes of (**A-D**) control and (**A′-D′**) *Jmjd5*$^{\Delta/\Delta}$ mouse embryos from E6.5 to E10.5. Scale bars: 400 μm.

Jmjd5$^{\Delta/\Delta}$ embryos could be detected from embryonic day (E) 6.5 to E11.5 (Fig. 1C and supplementary material Table S3), but were almost absorbed by E11.5 (5 of 5), suggesting that they died at ~E11.0.

At the same time, we analyzed the temporal and spatial expression pattern of endogenous *Jmjd5* during early embryogenesis. qRT-PCR analysis showed that *Jmjd5* was expressed at all embryonic stages examined (Fig. 1D), and the expression of *Jmjd5* was maintained at and just beyond the lethal stage (E11.0) of embryonic development. Whole-mount in situ hybridization (WISH) analysis using the antisense RNA probe for *Jmjd5* indicated that endogenous *Jmjd5* was ubiquitously expressed throughout the embryo at E8.5 (5 of 5; Fig. 1E, left), whereas the complementary sense RNA probe detected no signal (2 of 2; Fig. 1E, right). These results suggested an important role of *Jmjd5* during embryogenesis, at least after the post-implantation stages.

Next, we mated *Jmjd5*$^{+/\Delta}$ mice and dissected the pregnant mice to observe the phenotype of *Jmjd5*$^{\Delta/\Delta}$ embryos and littermates from E6.5 to E10.5 (Fig. 2). Although there was no phenotypic difference between *Jmjd5*$^{\Delta/\Delta}$ embryos and control littermates at E6.5 (8 of 8; Fig. 2A,A′), the growth of *Jmjd5*$^{\Delta/\Delta}$ embryos at E9.0 was obviously delayed compared with that of control embryos (8 of 8; Fig. 2B,B′). The *Jmjd5*$^{\Delta/\Delta}$ embryos at E9.0 looked similar to the wild-type embryos at E8.5. At this stage, we were unable to detect any other morphological defects in the appearance of *Jmjd5*$^{\Delta/\Delta}$ embryos. At E10.5, *Jmjd5*$^{\Delta/\Delta}$ embryos showed severe growth retardation, including incomplete embryonic turning. We also observed typical angiogenesis defects in *Jmjd5*$^{\Delta/\Delta}$ embryos, which had avascular yolk sacs (8 of 8; Fig. 2C′) and clumps of red blood cells (7 of 8; Fig. 2D′). This suggested that abnormal vascular development might lead to an insufficient circulatory system in *Jmjd5*$^{\Delta/\Delta}$ embryos, resulting in the observed embryonic growth retardation. However, a slight growth retardation of *Jmjd5*$^{\Delta/\Delta}$ embryos is already evident at E7.5, when endothelial precursors (angioblasts) start developing in the mouse embryo (data not shown). Thus, we concluded that Jmjd5 might be crucial for embryonic survival, especially for embryonic cell proliferation after the post-implantation stages.

Jmjd5 regulates the proliferation of MEFs

To examine whether Jmjd5 could intrinsically regulate embryonic cell proliferation, we attempted to prepare *Jmjd5*-deficient MEFs to examine the effect of Jmjd5 on cell growth. However, it was difficult to establish *Jmjd5*$^{\Delta/\Delta}$ MEFs because *Jmjd5*$^{\Delta/\Delta}$ embryos did not survive to E14.5, one of the most suitable stages for the preparation of MEFs. Interestingly, we found that the *Jmjd5*$^{neo/neo}$ homozygous mice also exhibited embryonic lethality without any excision of the *Jmjd5* allele (see Fig. 1 and supplementary material Table S4). At E10.5, whereas the majority of *Jmjd5*$^{neo/neo}$ embryos (25 of 37) showed severe growth retardation as observed for *Jmjd5*$^{\Delta/\Delta}$ embryos (supplementary material Fig. S1B), the 12 remaining *Jmjd5*$^{neo/neo}$ embryos seemed to be normal except for reduced body size (supplementary material Fig. S1C) and survived until E14.5. This result indicated that *Jmjd5*$^{neo/neo}$ embryos displayed a hypomorphic phenotype. Furthermore, RT-PCR analysis indicated that endogenous *Jmjd5* expression was significantly reduced in *Jmjd5*$^{neo/neo}$ embryos (supplementary material Fig. S2). Since *Jmjd5*$^{flox/flox}$ mice, in which the *Pgk-Neo* cassette has already been removed by mating with *CAG-Flp* mice, were viable and looked normal (data not shown), this suggested that the exogenous *Pgk-Neo* cassette from our targeting vector could be interfering with the expression of endogenous *Jmjd5*, resulting in the hypomorphic phenotype of *Jmjd5*$^{neo/neo}$ mice. Thus, we used these *Jmjd5*$^{neo/neo}$ embryos to establish *Jmjd5* hypomorphic MEFs for further analyses.

Pregnant mice were dissected at 14.5 days post-coitum and MEFs were prepared from each embryo. Genotypes were determined by PCR analysis and a single band of 0.5 kb, corresponding to the *Jmjd5*^{neo} allele, was detected for *Jmjd5*$^{neo/neo}$ MEFs (Fig. 3A). A ~75% reduction of endogenous *Jmjd5* expression was observed by qRT-PCR analysis in the prepared MEFs (Fig. 3B), and immunoblotting with anti-Jmjd5 antibody also showed that the expression of Jmjd5 was significantly lower than in wild type (Fig. 3C). Next, we compared cell growth between wild-type and *Jmjd5*$^{neo/neo}$ MEFs (Fig. 3D). The wild-type MEFs proliferated exponentially and became confluent after 72 hours in culture (n=3). However, the growth of *Jmjd5*$^{neo/neo}$ MEFs was significantly reduced compared with wild-type MEFs within 48 hours of passage (n=3, P<0.01), and the cell number decreased to ~50% of that of control cells 72 hours after passage (Fig. 3D). This result suggested that Jmjd5 plays an important role in embryonic cell proliferation.

To examine whether the decreased cell number of *Jmjd5*$^{neo/neo}$ MEFs might be due to induced premature senescence, we carried out senescence-associated β-galactosidase staining. β-galactosidase-positive cells were not detected in *Jmjd5*$^{neo/neo}$ or

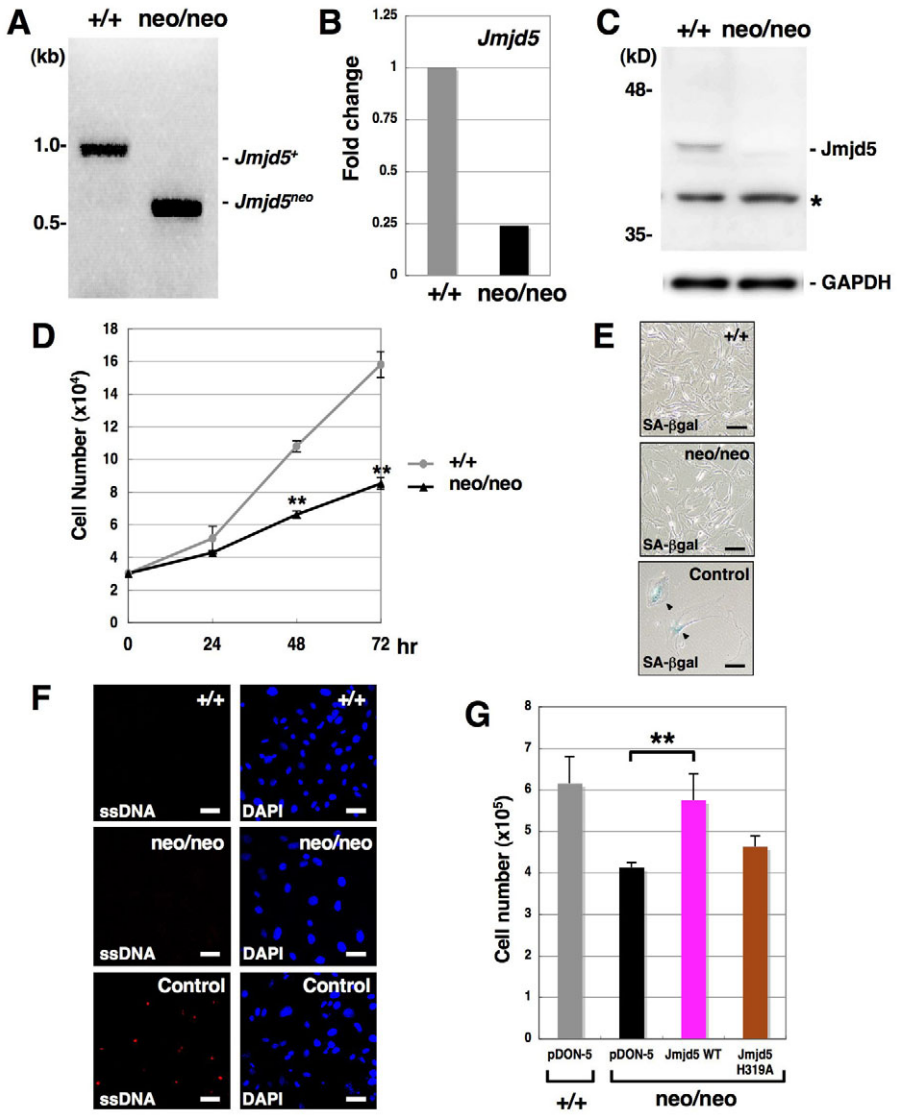

Fig. 3. *Jmjd5*$^{neo/neo}$ hypomorphic mouse embryonic fibroblasts (MEFs) proliferate more slowly than wild-type MEFs. (**A**) Genotyping PCR using genomic DNA from *Jmjd5*$^{+/+}$ or *Jmjd5*$^{neo/neo}$ MEFs. (**B**) qRT-PCR analysis of *Jmjd5* expression in *Jmjd5*$^{+/+}$ or *Jmjd5*$^{neo/neo}$ MEFs. (**C**) Immunoblotting with anti-Jmjd5 antibody showed significant reduction of endogenous Jmjd5 protein in *Jmjd5*$^{neo/neo}$ MEFs. Asterisk marks a non-specific band. (**D**) Growth curve for *Jmjd5*$^{+/+}$ or *Jmjd5*$^{neo/neo}$ MEFs. The mean ± s.d. from at least three experiments is shown; $^{**}P<0.01$, Student's *t*-test. (**E**) Senescence-associated β-galactosidase (SA-βgal) assays for *Jmjd5*$^{+/+}$ (top) and *Jmjd5*$^{neo/neo}$ (middle) MEFs. As a positive control for the detection of senescent cells, sparsely seeded MEFs were stained (bottom). (**F**) Immunofluorescence assay with anti-ssDNA antibody for *Jmjd5*$^{+/+}$ (top) or *Jmjd5*$^{neo/neo}$ (middle) MEFs. The cells were treated with anti-ssDNA antibody (left) and counterstained with DAPI (right). As a positive control, MEFs treated with adriamycin were stained (bottom). (**G**) The growth defect of *Jmjd5*$^{neo/neo}$ MEFs was rescued by the re-expression of wild-type Jmjd5. The *Jmjd5*$^{neo/neo}$ or *Jmjd5*$^{+/+}$ MEFs were infected with retrovirus without insert (pDON-5) or expressing wild-type Jmjd5 or the H319A mutant. The cell number was counted 48 hours after infection. $^{**}P<0.01$. Scale bars: 100 μm in E; 50 μm in F.

wild-type MEFs (Fig. 3E, middle and top), although β-galactosidase-positive cells could clearly be detected in the control sparsely seeded MEFs (Fig. 3E, bottom). Next, we performed an immunofluorescence assay with anti-single-stranded DNA (ssDNA) antibody to examine whether the cells undergo apoptosis at a higher rate. Whereas many cells were stained with anti-ssDNA antibody in the positive controls (adriamycin-treated MEFs; Fig. 3F, bottom), we did not observe an elevated occurrence of ssDNA-positive cells in *Jmjd5*$^{neo/neo}$ MEFs as compared with wild-type MEFs (Fig. 3F, middle and top). These results indicated that downregulation of Jmjd5 did not increase premature senescence and apoptosis, but rather decreased embryonic cell proliferation.

Next we examined whether the growth retardation of *Jmjd5*$^{neo/neo}$ MEFs was dependent on Jmjd5 demethylase activity. The *Jmjd5*$^{neo/neo}$ MEFs were infected with control retrovirus or with retrovirus expressing wild-type Jmjd5 or the catalytically inactive mutant H319A. The expression of *Jmjd5* was increased to the same level when MEFs were infected with virus expressing wild-type or inactive Jmjd5 (supplementary material Fig. S3). MEF cell number was counted 48 hours after infection, and the cell growth defect of *Jmjd5*$^{neo/neo}$ MEFs was significantly rescued by re-expressing wild-type Jmjd5 (Fig. 3G). No significant change was observed with the expression of the inactive H319A mutant as compared with the control. These results suggested that the demethylase activity of Jmjd5 is required for normal embryonic cell proliferation.

The expression of *Cdkn1a* (*p21*) is upregulated in *Jmjd5*$^{neo/neo}$ MEFs and *Jmjd5*$^{Δ/Δ}$ embryos

A recent report showed that JMJD5 activated the expression of the *CCNA1* gene in MCF7 breast cancer cells by demethylating H3K36me2 on the *CCNA1* locus, resulting in cell cycle progression (Hsia et al., 2010). Thus, we first examined whether loss of Jmjd5 caused the downregulation of *Ccna1* in mouse embryonic cells. We extracted total RNA from *Jmjd5*$^{neo/neo}$ MEFs or *Jmjd5*$^{Δ/Δ}$ embryos to synthesize cDNA and performed qRT-PCR analysis using *Ccna1*-specific primers. Unexpectedly, there was no change in the expression of *Ccna1* in *Jmjd5*$^{neo/neo}$ MEFs or *Jmjd5*$^{Δ/Δ}$ embryos as compared with wild type (Fig. 4A,D). This indicated that there might be a different regulatory function of Jmjd5 in mouse embryonic cells and human cancer cell lines.

Various genetic studies using knockout mice have shown that a number of cell cycle regulators are involved in normal mouse development (Ciemerych and Sicinski, 2005). Therefore, we

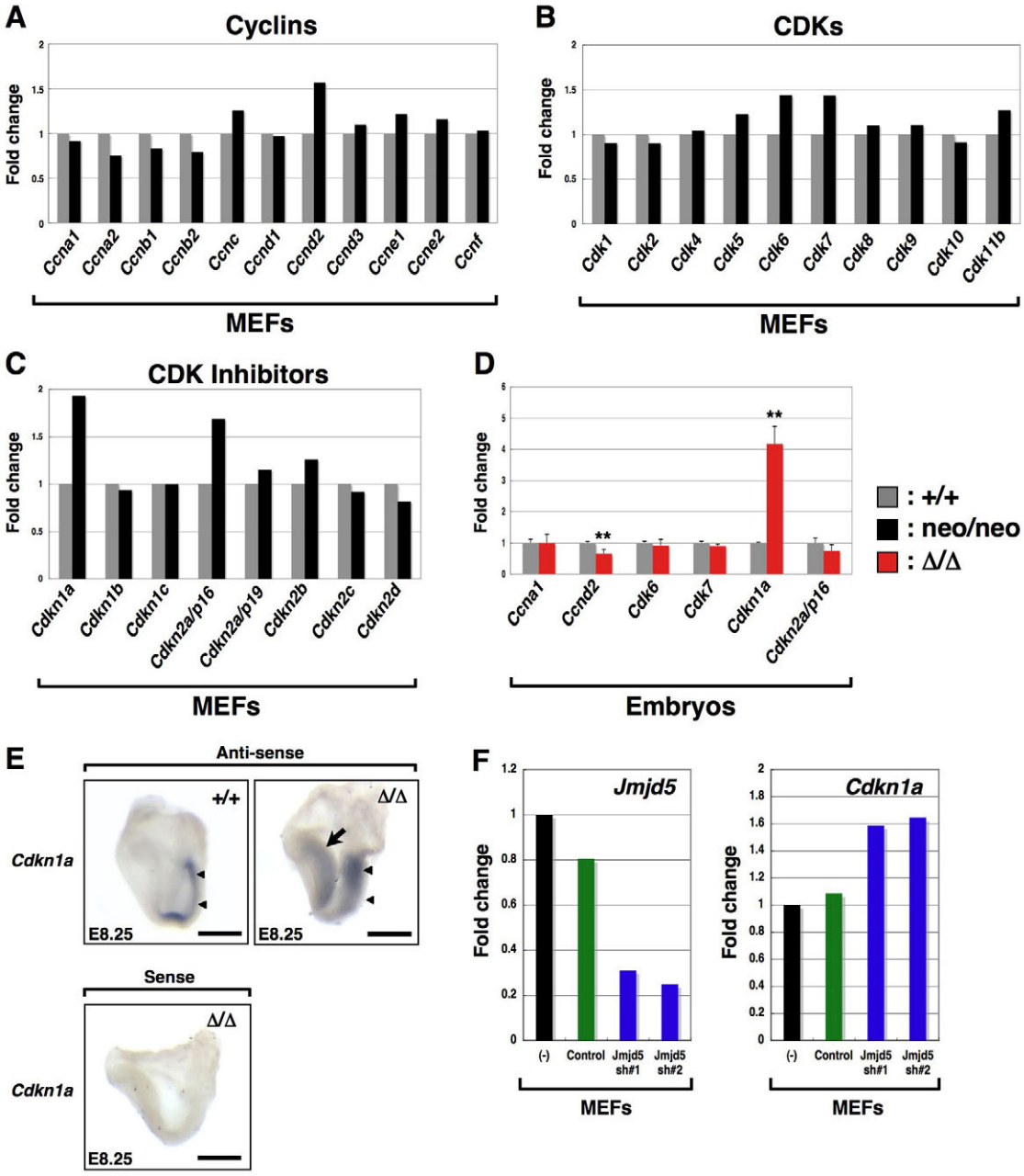

Fig. 4. Expression of *Cdkn1a* is upregulated in *Jmjd5*-deficient cells. (**A-C**) The expression of cyclins (A), CDKs (B) and CDK inhibitors (C) in *Jmjd5*$^{+/+}$ (gray bar) and *Jmjd5*$^{neo/neo}$ (black bar) MEFs as detected by qRT-PCR. (**D**) The expression of *Ccna1*, *Ccnd2*, *Cdk6*, *Cdk7*, *Cdkn1a* and *Cdkn2a* in *Jmjd5*$^{+/+}$ embryos at E8.25 (gray bar) and stage-matched *Jmjd5*$^{\Delta/\Delta}$ embryos (red bar). The mean ± s.d. from at least three experiments is shown. $^{**}P<0.01$. (**E**) WISH analysis of *Jmjd5*$^{+/+}$ and *Jmjd5*$^{\Delta/\Delta}$ embryos with the sense or antisense probe for *Cdkn1a*. Arrowheads indicate the primitive streak and the arrow indicates the ectopic expression of *Cdkn1a* in the anterior half. Scale bars: 400 μm. (**F**) qRT-PCR analysis of *Jmjd5* and *Cdkn1a* transcripts in MEFs after knockdown of *Jmjd5*. (–) indicates uninfected MEFs.

attempted to examine whether the loss of Jmjd5 affected the expression of representative cell cycle regulators, including eleven cyclins, ten CDKs, eight CDK inhibitors and Rb family members, during mouse embryogenesis. The expression of *Ccnd2*, *Cdk6* and *Cdk7* was 1.57-fold, 1.44-fold and 1.43-fold higher, respectively, in *Jmjd5*$^{neo/neo}$ than in wild-type MEFs (Fig. 4A,B). In addition, the expression of *Cdkn1a* and *Cdkn2a* (*p16Ink4a*) was 1.93-fold and 1.69-fold higher, respectively, than in wild type, (Fig. 4C). By contrast, the expression of other cyclins, CDKs, CDK inhibitors and the Rb family members was not significantly changed in *Jmjd5*$^{neo/neo}$ MEFs (Fig. 4A-C and supplementary material Fig. S4). Next, we examined the expression of *Ccnd2*, *Cdk6*, *Cdk7*, *Cdkn1a* and *Cdkn2a* in wild-type embryos at the early somite stage (E8.25, n=3) and in stage-matched *Jmjd5*$^{\Delta/\Delta}$ embryos (n=7) by qRT-PCR analysis. In agreement with our data from *Jmjd5*$^{neo/neo}$ MEFs, we detected a significant increase of *Cdkn1a* transcripts (4.17-fold, $P<0.01$) in *Jmjd5*$^{\Delta/\Delta}$ embryos (Fig. 4D). However, unlike the upregulation in *Jmjd5*$^{neo/neo}$ MEFs, the expression of other candidates was not altered in *Jmjd5*$^{\Delta/\Delta}$ embryos, and the expression of *Ccnd2* showed a 1.52-fold reduction ($P<0.01$). Since *Cdkn1a*

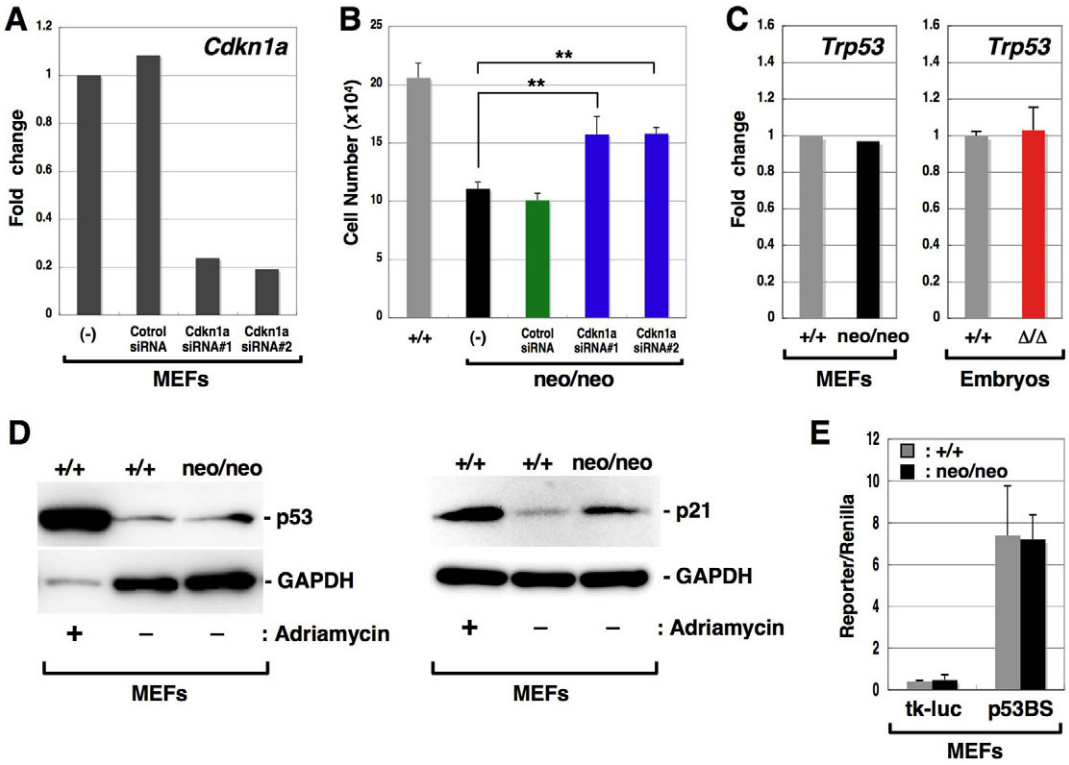

Fig. 5. Jmjd5 intrinsically regulates the expression of *Cdkn1a* without the transcriptional activation of p53. (**A**) qRT-PCR analysis for the validation of *Cdkn1a*-specific siRNAs. (**B**) Comparative growth assay between control and *Cdkn1a* knockdown *Jmjd5*$^{neo/neo}$ MEFs. Cell number was counted 72 hours after passage for *Jmjd5*$^{+/+}$ (gray bar), *Jmjd5*$^{neo/neo}$ (black bar), control siRNA-treated (green bar) or *Cdkn1a*-specific siRNA-treated *Jmjd5*$^{neo/neo}$ (blue bar) MEFs. The mean ± s.d. from at least three experiments is shown. **P<0.01. (**C**) qRT-PCR analysis for the detection of *p53* (*Trp53*) in MEFs and E8.25 embryos. (**D**) Immunoblotting with anti-p53 antibody (left) or anti-Cdkn1a (p21) (right). The lysate of adriamycin-treated wild-type MEFs was used as a positive control for the induction of p53 (one-quarter the amount of the samples) or Cdkn1a (the same amount as the samples) protein. Anti-Gapdh antibody was used for loading controls. (**E**) Luciferase assay with the *tk* promoter luciferase vector (tk-luc) or p53-responsive luciferase vector (p53BS) showed no significant difference between wild-type and *Jmjd5*$^{neo/neo}$ MEFs.

expression was commonly elevated in both *Jmjd5*$^{neo/neo}$ MEFs and *Jmjd5*$^{\Delta/\Delta}$ embryos, we selected *Cdkn1a* as a probable transcriptional target of Jmjd5.

To evaluate the spatial alteration of *Cdkn1a* expression in *Jmjd5*$^{\Delta/\Delta}$ embryos, we also performed WISH analysis (Fig. 4E). The elevation of *Cdkn1a* was detected in the posterior half of the *Jmjd5*$^{\Delta/\Delta}$ embryo including the primitive streak, where endogenous *Cdkn1a* was highly expressed in the wild-type embryo. Ectopic expression of *Cdkn1a* was also observed in the anterior half of the *Jmjd5*$^{\Delta/\Delta}$ embryo (7 of 10). A complementary sense probe for *Cdkn1a* was unable to detect any signals (4 of 4). These results suggested that endogenous Jmjd5 could be responsible for the spatial expression pattern of *Cdkn1a* in whole embryos.

Next we examined whether knockdown of *Jmjd5* expression could induce upregulation of *Cdkn1a*. We used retroviruses expressing two different small hairpin RNAs (shRNAs) for *Jmjd5* (*Jmjd5* sh#1 and sh#2). MEFs were infected with control retrovirus or retrovirus expressing each *Jmjd5* shRNA. qRT-PCR indicated that *Jmjd5* transcripts were significantly reduced upon infection with either *Jmjd5* shRNA-expressing retrovirus, but not with the control retrovirus (Fig. 4F, left). We then examined the effect of *Jmjd5* knockdown on the expression of *Cdkn1a*. Both *Jmjd5*-specific shRNAs led to a significant increase in *Cdkn1a* transcripts (1.59-fold and 1.65-fold; Fig. 4F, right). These observations suggested that Jmjd5 might be directly involved in the regulation of *Cdkn1a* expression in MEFs.

Jmjd5 regulates the expression of *Cdkn1a* intrinsically, without stimulation of the p53-p21 pathway

According to the results shown in Figs 3 and 4, we speculated that *Cdkn1a* upregulation caused by the reduction in *Jmjd5* levels might underlie the observed growth retardation. To test our hypothesis, we performed a knockdown assay using *Cdkn1a*-specific siRNAs and investigated whether the reduction of *Cdkn1a* could rescue the inhibition of cell proliferation in *Jmjd5*$^{neo/neo}$ MEFs. Two *Cdkn1a*-specific siRNAs (siRNA#1 and #2) were designed, and the knockdown efficiency of each siRNA was shown to be ~80% (Fig. 5A). *Cdkn1a* siRNA#1, #2 or an unrelated control siRNA was transfected into *Jmjd5*$^{neo/neo}$ MEFs and their growth compared. Knockdown of *Cdkn1a* in *Jmjd5*$^{neo/neo}$ MEFs caused a significant increase in cell proliferation as compared with that of *Jmjd5*$^{neo/neo}$ MEFs treated with the control siRNA or untreated *Jmjd5*$^{neo/neo}$ MEFs (n=3, P<0.01; Fig. 5B). The cell number of *Jmjd5*$^{neo/neo}$ MEFs treated with the *Cdkn1a*-specific siRNAs was still lower than that of wild-type MEFs, indicating a partial rescue of cell growth by *Cdkn1a* knockdown. These results suggested that the regulation of *Cdkn1a* expression by Jmjd5 plays an important, but not exclusive, role in embryonic cell proliferation, although incomplete knockdown of *Cdkn1a* might also be responsible for the partial rescue phenotype.

Since it is known that *Cdkn1a* is a major direct target for the p53 (Trp53) pathway (Wood and Shilatifard, 2006), we examined whether the elevation of *Cdkn1a* was dependent on the induction

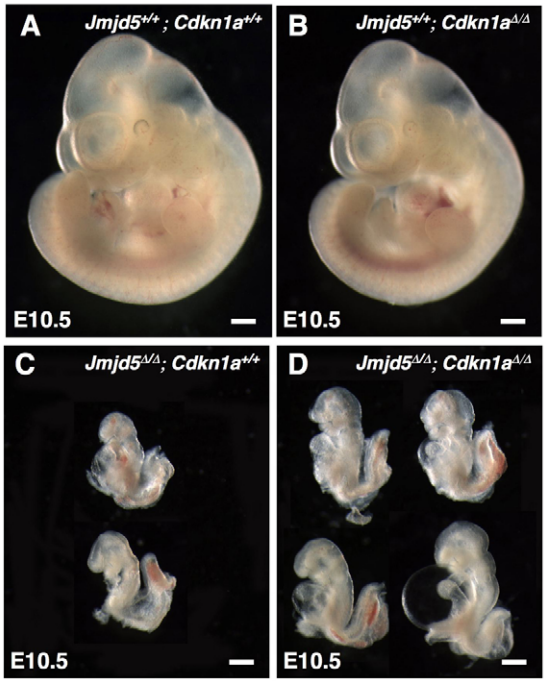

Fig. 6. Phenotypic analysis of *Jmjd5*$^{\Delta/\Delta}$; *Cdkn1a*$^{\Delta/\Delta}$ double-knockout embryos. *Jmjd5*$^{+/\Delta}$; *Cdkn1a*$^{+/\Delta}$ double-heterozygous mice were intercrossed. (**A**) Wild-type, (**B**) *Cdkn1a*-deficient, (**C**) *Jmjd5*-deficient and (**D**) *Jmjd5*$^{\Delta/\Delta}$; *Cdkn1a*$^{\Delta/\Delta}$ embryos were observed at E10.5. Scale bars: 500 μm.

of endogenous *p53* transcripts in *Jmjd5*-deficient cells. qRT-PCR showed that there was no difference in the expression of *p53* in *Jmjd5*$^{neo/neo}$ MEFs and *Jmjd5*$^{\Delta/\Delta}$ embryos as compared with control cells (Fig. 5C). Immunoblotting also indicated that there was no alteration in the level of p53 protein between wild-type and *Jmjd5*$^{neo/neo}$ MEFs, despite the enrichment of Cdkn1a (p21) protein in *Jmjd5*$^{neo/neo}$ MEFs (Fig. 5D). We next measured the transcriptional activity of p53 in wild-type and *Jmjd5*$^{neo/neo}$ MEFs by luciferase assay. We constructed a *p53BS-tk*-luciferase reporter (p53BS) containing p53 response elements derived from human *CDKN1A* (El-Deiry et al., 1993), and transfected the reporter or control plasmid (tk-luc) together with a *Renilla* luciferase reference plasmid into wild-type or *Jmjd5*$^{neo/neo}$ MEFs. There was no significant difference in the luciferase activity (n=4; Fig. 5E), indicating that an alteration in p53 transcriptional activity did not occur in *Jmjd5*$^{neo/neo}$ MEFs.

We then investigated whether the growth retardation caused by the loss of Jmjd5 was closely associated with the dysregulation of *Cdkn1a* in these embryos. *Jmjd5*-deficient mice were intercrossed with *Cdkn1a*-deficient mice (*Cdkn1a*$^{\Delta/\Delta}$), which were morphologically normal at E10.5 (5 of 5; Fig. 6B) (Deng et al., 1995), to generate *Jmjd5* and *Cdkn1a* double-knockout mice (*Jmjd5*$^{\Delta/\Delta}$; *Cdkn1a*$^{\Delta/\Delta}$). Phenotypes were compared between the double-knockout and *Jmjd5*-deficient mice. As with *Jmjd5*$^{\Delta/\Delta}$ mice, the *Jmjd5*$^{\Delta/\Delta}$; *Cdkn1a*$^{\Delta/\Delta}$ genotype was embryonic lethal (data not shown) and the mice showed the severe growth retardation (4 of 4; Fig. 6D) as compared with wild-type embryos (Fig. 6A). However, *Jmjd5*$^{\Delta/\Delta}$; *Cdkn1a*$^{\Delta/\Delta}$ embryos were slightly larger than *Jmjd5*$^{\Delta/\Delta}$ littermates (Fig. 6C). Other abnormal phenotypes, such as the incomplete turning and the angiogenesis defect, did not seem to be rescued in the double-knockout embryos. These results suggested that the deficiency of *Cdkn1a* could partially rescue the phenotype of *Jmjd5*$^{\Delta/\Delta}$ embryos, similar to our result from the knockdown experiment (Fig. 5B). We therefore demonstrated that a genetic interaction between *Jmjd5* and *Cdkn1a* is at least important for embryonic cell proliferation, but also propose that other factors regulated by Jmjd5 contribute to normal embryonic cell growth.

Jmjd5 is involved in the maintenance of H3K36me2 at the *Cdkn1a* locus

Previous studies suggested that Jmjd5 is an H3K36me2 histone demethylase (Hsia et al., 2010) and that methylated K36 in histone H3 is an active transcriptional mark (Li et al., 2007). Thus, we assumed that the loss of Jmjd5 caused an elevation of H3K36me2 at the *Cdkn1a* locus, resulting in the activation of *Cdkn1a* in *Jmjd5*-deficient cells. To test our hypothesis, we designed primers to amplify several genomic regions of *Cdkn1a* for chromatin immunoprecipitation (ChIP) analysis (Fig. 7A). The crosslinked chromatin from wild-type or *Jmjd5*$^{neo/neo}$ MEFs was immunoprecipitated with anti-K36me2 or anti-Jmjd5 antibody and the precipitates were used for the detection of *Cdkn1a* genomic regions by qPCR. Enrichment of H3K36me2 was observed in intron II (regions a and b) and exon III (region c containing the open reading frames of *Cdkn1a*) but not in intron III (region d) of *Cdkn1a* (n>9, P<0.01) in *Jmjd5*$^{neo/neo}$ MEFs (Fig. 7B). The recruitment of Jmjd5 to the *Cdkn1a* locus was significantly reduced in regions a, b and c, whereas no significant change was observed in region d (n>9, P<0.01; Fig. 7C). These results suggested that reduced recruitment of Jmjd5 to several regions of the *Cdkn1a* locus induced increased H3K36me2. Based on the previous report showing a correlation between enriched H3K36me2 and the transcriptionally active phase (Li et al., 2007), one may propose that the increased H3K36me2 induces *Cdkn1a* expression in *Jmjd5*$^{neo/neo}$ MEFs.

We also performed ChIP analysis with anti-H3K4me3 antibody to investigate whether another epigenetic mark, H3K4me3, was altered in regions a, b and c of *Cdkn1a*. Enrichment of H3K4me3 was observed only in region a, whereas significant changes were not detected in the other regions (supplementary material Fig. S5). Since H3K4me3 is an active transcriptional mark (Martin and Zhang, 2005), this alteration of H3K4me3 in a Jmjd5-independent manner might reflect the enhanced transcriptional activation of *Cdkn1a* in *Jmjd5*$^{neo/neo}$ MEFs. Taken together, our data demonstrate that *Cdkn1a* is one of the downstream targets of Jmjd5 histone demethylase and that the maintenance of H3K36me2 at the *Cdkn1a* locus, as regulated by Jmjd5, might be required for normal embryonic proliferation.

DISCUSSION

In this study, we generated *Jmjd5*-deficient mice and observed severe growth retardation in *Jmjd5*$^{\Delta/\Delta}$ embryos, leading to embryonic lethality at ~E11.0. In *Jmjd5*$^{\Delta/\Delta}$ embryos, significant upregulation of *Cdkn1a* was detected. Similarly, growth retardation as well as elevated expression of *Cdkn1a* were observed in *Jmjd5*$^{neo/neo}$ MEFs. ChIP analysis indicated that, in *Jmjd5*$^{neo/neo}$ MEFs, H3K36me2 was significantly increased in several regions of the *Cdkn1a* locus where the recruitment of endogenous Jmjd5 was reduced. Thus, we demonstrate for the first time that Jmjd5 moderates the expression of *Cdkn1a* during embryogenesis through histone demethylase activity.

Currently, there are more than 30 known mammalian JmjC domain-encoding genes, and some have been reported to be involved in cell proliferation by regulating the expression of cell

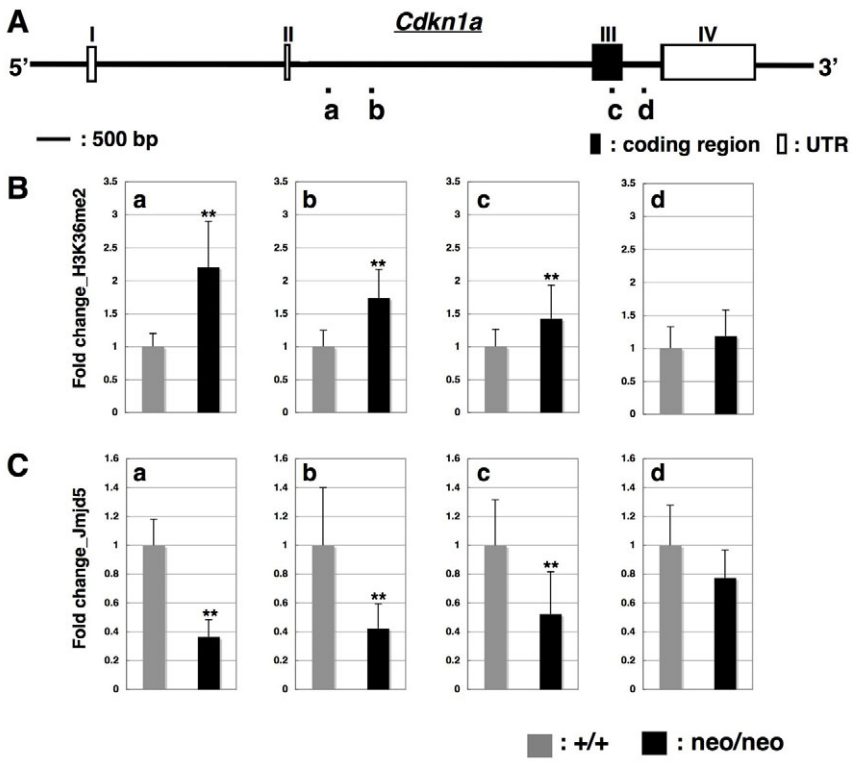

Fig. 7. Elevated level of H3K36me2 and decreased recruitment of Jmjd5 at the *Cdkn1a* locus of *Jmjd5*$^{neo/neo}$ MEFs. (**A**) The *Cdkn1a* locus and the distribution of amplified regions (a to d) for ChIP analysis. (**B**) ChIP analysis with anti-H3K36me2 antibody to determine the sites of H3K36me2 enrichment in the four regions of the *Cdkn1* locus in *Jmjd5*$^{neo/neo}$ MEFs (black bar), as compared with wild-type MEFs (gray bar). (**C**) ChIP analysis with anti-Jmjd5 antibody to detect the recruitment of endogenous Jmjd5. The mean ± s.d. from at least nine experiments is shown. $^{**}P<0.01$.

cycle inhibitors. Our recent study demonstrated that Kdm6a directly demethylates H3K27me3 in *Rb1* and *Rbl2*, increasing their expression levels and resulting in the growth repression of MEFs (Terashima et al., 2010). KDM6B (JMJD3), an H3K27 demethylase, activated the *INK4A-ARF* locus in response to oncogenic stress, and its overexpression led to the inhibition of cell proliferation (Agger et al., 2009; Barradas et al., 2009). Furthermore, Kdm2b, an H3K36 demethylase, regulated cell proliferation through the modulation of *Cdkn2b* (He et al., 2008). These results strongly suggest that the JmjC family plays an essential role in cell growth signaling. Our analysis with *Jmjd5*-deficient mice indicated a novel association of *Jmjd5* and *Cdkn1a* expression that is crucial for cell proliferation during normal mouse development.

Genome-wide profiling of methylated histone H3 from yeast to humans showed that H3K36 methylation tended to be enriched across the transcribed regions of active genes rather than promoter regions (Li et al., 2007). In *Saccharomyces cerevisiae*, methylation of histone H3 by Set2, an H3K36 KMT, is associated with transcriptional elongation by RNA polymerase II (Krogan et al., 2003; Schaft et al., 2003). However, there is still little evidence for the physiological function of H3K36me2 in mammals. Recently, knockdown of *Kdm2b* in MEFs was shown to induce the activation of *Cdkn2b* by increased H3K36me2 at the *Cdkn2b* locus (He et al., 2008). Our study demonstrated that the disruption of *Jmjd5* in mouse cells induced *Cdkn1a* transcription and the elevation of H3K36me2 at the transcribed regions of *Cdkn1a*, supporting the current model linking transcriptional activation and methylated H3K36.

We observed the induced expression of *Cdkn1a* in *Jmjd5*$^{\Delta/\Delta}$ embryos and *Jmjd5*$^{neo/neo}$ MEFs. Although *Cdkn1a* is a p53 target gene, we did not detect any significant changes in p53 expression at either the transcriptional or translational level. The reporter assay showed that the transcriptional activity of p53 was not changed in *Jmjd5*$^{neo/neo}$ MEFs, and immunofluorescence and immunoprecipitation studies indicated no alteration in the subcellular localization of p53 and no direct interaction between Jmjd5 and p53 (data not shown). These results suggested that the aberrant induction of *Cdkn1a* seemed to occur without p53 induction. However, we cannot exclude the possibility that p53 signaling is altered, as the p53 protein receives various post-translational modifications, such as phosphorylation, methylation, acetylation and ubiquitylation, which affect its stability, specificity for target genes and affinity for co-factors (Carter and Vousden, 2009). Therefore, more detailed analyses would be necessary to prove whether there is a connection between Jmjd5 and p53.

In all of the *Jmjd5*$^{\Delta/\Delta}$ embryos examined, severe growth retardation was observed, and the expression of *Cdkn1a* was more than 4-fold higher than in wild-type embryos. However, growth retardation is sometimes caused indirectly by abnormal placental development in genetically modified mice (Han and Carter, 2001). In fact, endogenous *Jmjd5* expression was detected in the ectoplacental cone, a precursor of the placenta, at E8.5. The allantois needs to fuse with the chorion for normal placental development, but this was not observed in some *Jmjd5*$^{\Delta/\Delta}$ embryos at E10.5 (3 of 8; data not shown). Thus, we could not exclude the possibility that abnormal placental development might be a reason for the growth defect in *Jmjd5*$^{\Delta/\Delta}$ embryos. However, it was notable that high expression of endogenous *Jmjd5* was observed in not only the ectoplacental cone but also the entire embryonic fraction. We also demonstrated that although embryonic cells purified from *Jmjd5*$^{neo/neo}$ embryos are not under placental control, these cells still showed the defect in proliferation and the elevated expression of *Cdkn1a*. Furthermore, knockdown of endogenous *Cdkn1a* was able to rescue the growth delay significantly in *Jmjd5*$^{neo/neo}$ MEFs. The growth retardation in *Jmjd5*$^{\Delta/\Delta}$ embryos was also partially rescued in the *Cdkn1a*$^{\Delta/\Delta}$ genetic background. These results indicated that the regulation of *Cdkn1a* by Jmjd5 played an

important role in cell proliferation and embryonic development. Since the rescue effect was partial, this suggests that additional factors regulated by Jmjd5 contribute to embryonic development. We are now trying to identify other target genes that are regulated by Jmjd5 by microarray and ChIP-sequence, and hope to reveal the detailed mechanism of Jmjd5 function in embryonic cell proliferation in the near future.

Similar to the phenotype observed in *Jmjd5*$^{\Delta/\Delta}$ embryos, the upregulation of endogenous *Cdkn1a* has been reported in several mutant mice, resulting in severe growth retardation (Ruland et al., 2001; Rantakari et al., 2010; Suzuki et al., 1997). Notably, the elevation of *Cdkn1a* in *Brca1*- or *Mdm4*-deficient mice has been observed (Hakem et al., 1996; Migliorini et al., 2002), and, importantly, intercrossing with *Cdkn1a*-deficient mice partially rescued the phenotype, suggesting that the aberrant expression of *Cdkn1a* is a major, but not exclusive, reason for the embryonic death (Hakem et al., 1997; Steinman et al., 2004). Interestingly, the phenotype of histone deacetylase 1 (*Hdac1*)-deficient mice was similar, although more severe, than with *Jmjd5*$^{\Delta/\Delta}$ mice. Disruption of *Hdac1* resulted in lethality before E10.5 due to severe growth retardation, and the expression of *Cdkn1a* and *Cdkn1b* was upregulated (Lagger et al., 2002). This result suggested that several epigenetic controls, including histone methylation and acetylation, are closely associated with the normal expression of *Cdkn1a* during embryogenesis. Therefore, clarification of the relationship between Jmjd5 and other histone-modifying enzymes would be helpful for understanding the detailed mechanism of *Cdkn1a* regulation by Jmjd5.

Acknowledgements

We thank Dr N. Nozaki (Hokkaido University, Japan) for providing anti-di-methylated H3K36 antibody; Drs J. Takeda (Osaka University, Japan), N. A. Jenkins and N. G. Copeland (IMCB, Singapore) for providing gene targeting vectors; Drs Y. Nakanishi and K. Yoshioka (Kanazawa University, Japan) for providing *Pgk2-Cre* transgenic mice; Dr S. Itohara (RIKEN, Japan) for *CAG-Flp* transgenic mice; and Dr A. Hirao (Kanazawa University, Japan) for *Cdkn1a*-deficient mice.

Funding

This study was supported by a Grant-in-Aid for Young Scientist (B) [23790220 to A.I.] and Scientific Research (C) [21590303 to T.S.] from the Ministry of Education, Culture, Sports, Science and Technology of Japan.

Competing interests statement

The authors declare no competing financial interests.

Supplementary material

Supplementary material available online at
http://dev.biologists.org/lookup/suppl/doi:10.1242/dev.074138/-/DC1

References

Abidi, F. E., Miano, M. G., Murray, J. C. and Schwartz, C. E. (2007). A novel mutation in the PHF8 gene is associated with X-linked mental retardation with cleft lip/cleft palate. *Clin. Genet.* **72**, 19-22.

Agger, K., Cloos, P. A., Rudkjaer, L., Williams, K., Andersen, G., Christensen, J. and Helin, K. (2009). The H3K27me3 demethylase JMJD3 contributes to the activation of the *INK4A-ARF* locus in response to oncogene- and stress-induced senescence. *Genes Dev.* **23**, 1171-1176.

Ando, H., Haruna, Y., Miyazaki, J., Okabe, M. and Nakanishi, Y. (2000). Spermatocyte-specific gene excision by targeted expression of Cre recombinase. *Biochem. Biophys. Res. Commun.* **272**, 125-128.

Barradas, M., Anderton, E., Acosta, J. C., Li, S., Banito, A., Rodriguez-Niedenführ, M., Maertens, G., Banck, M., Zhou, M. M., Walsh, M. J. et al. (2009). Histone demethylase JMJD3 contributes to epigenetic control of *INK4a/ARF* by oncogenic RAS. *Genes Dev.* **23**, 1177-1182.

Carter, S. and Vousden, K. H. (2009). Modifications of p53: competing for the lysines. *Curr. Opin. Genet. Dev.* **19**, 18-24.

Ciemerych, M. A. and Sicinski, P. (2005). Cell cycle in mouse development. *Oncogene* **24**, 2877-2898.

Deng, C., Zhang, P., Harper, J. W., Elledge, S. J. and Leder, P. (1995). Mice lacking p21CIP1/WAF1 undergo normal development, but are defective in G1 checkpoint control. *Cell* **82**, 675-684.

Eggan, K,., Akutsu, H., Loring, J., Jackson-Grusby, L., Klemm, M., Rideout, W. M., 3rd, Yanagimachi, R. and Jaenisch, R. (2001). Hybrid vigor, fetal overgrowth, and viability of mice derived by nuclear cloning and tetraploid embryo complementation. *Proc. Natl. Acad. Sci. USA* **98**, 6209-6214.

Ehrbrecht, A., Müller, U., Wolter, M., Hoischen, A., Koch, A., Radlwimmer, B., Actor, B., Mincheva, A., Pietsch, T., Lichter, P. et al. (2006). Comprehensive genomic analysis of desmoplastic medulloblastomas: identification of novel amplified genes and separate evaluation of the different histological components. *J. Pathol.* **208**, 554-563.

El-Deiry, W. S., Tokino, T., Velculescu, V. E., Levy, D. B., Parsons, R., Trent, J. M., Lin, D., Mercer, W. E., Kinzler, K. W. and Vogelstein, B. (1993). *WAF1*, a potential mediator of p53 tumor suppression. *Cell* **75**, 817-825.

Fukuda, T., Tokunaga, A., Sakamoto, R. and Yoshida, N. (2011). Fbxl10/Kdm2b deficiency accelerates neural progenitor cell death and leads to exencephaly. *Mol. Cell. Neurosci.* **46**, 614-624.

Hakem, R., de la Pompa, J. L., Sirard, C., Mo, R., Woo, M., Hakem, A., Wakeham, A., Potter, J., Reitmair, A., Billia, F. et al. (1996). The tumor suppressor gene *Brca1* is required for embryonic cellular proliferation in the mouse. *Cell* **85**, 1009-1023.

Hakem, R., de la Pompa, J. L., Elia, A., Potter, J. and Mak, T. W. (1997). Partial rescue of *Brca1 (5-6)* early embryonic lethality by *p53* or *p21* null mutation. *Nat. Genet.* **16**, 298-302.

Han, V. K. and Carter, A. M. (2001). Control of growth and development of the feto-placental unit. *Curr. Opin. Pharmacol.* **1**, 632-640.

Hayami, S., Yoshimatsu, M., Veerakumarasivam, A., Unoki, M., Iwai, Y., Tsunoda, T., Field, H. I., Kelly, J. D., Neal de Yamaue, H. et al. (2010). Overexpression of the JmjC histone demethylase KDM5B in human carcinogenesis: involvement in the proliferation of cancer cells through the E2F/RB pathway. *Mol. Cancer* **9**, 59.

He, J., Kallin, E. M., Tsukada, Y. and Zhang, Y. (2008). The H3K36 demethylase Jhdm1b/Kdm2b regulates cell proliferation and senescence through p15(Ink4b). *Nat. Struct. Mol. Biol.* **15**, 1169-1175.

Hsia, D. A., Tepper, C. G., Pochampalli, M. R., Hsia, E. Y., Izumiya, C., Huerta, S. B., Wright, M. E., Chen, H. W., Kung, H. J. and Izumiya, Y. (2010). KDM8, a H3K36me2 histone demethylase that acts in the cyclin A1 coding region to regulate cancer cell proliferation. *Proc. Natl. Acad. Sci. USA* **107**, 9671-9676.

Inagaki, T., Tachibana, M., Magoori, K., Kudo, H., Tanaka, T., Okamura, M., Naito, M., Kodama, T., Shinkai, Y. and Sakai, J. (2009). Obesity and metabolic syndrome in histone demethylase JHDM2a-deficient mice. *Genes Cells* **14**, 991-1001.

Jensen, L. R., Amende, M., Gurok, U., Moser, B., Gimmel, V., Tzschach, A., Janecke, A. R., Tariverdian, G., Chelly, J., Fryns, J. P. et al. (2005). Mutations in the *JARID1C* gene, which is involved in transcriptional regulation and chromatin remodeling, cause X-linked mental retardation. *Am. J. Hum. Genet.* **76**, 227-236.

Jones, M. A., Covington, M. F., DiTacchio, L., Vollmers, C., Panda, S. and Harmer, S. L. (2010). Jumonji domain protein JMJD5 functions in both the plant and human circadian systems. *Proc. Natl. Acad. Sci. USA* **107**, 21623-21628.

Kanki, H., Suzuki, H. and Itohara, S. (2006). High-efficiency CAG-FLPe deleter mice in C57BL/6J background. *Exp. Anim.* **55**, 137-141.

Kimura, H., Hayashi-Takanaka, Y., Goto, Y., Takizawa, N. and Nozaki, N. (2008). The organization of histone H3 modifications as revealed by a panel of specific monoclonal antibodies. *Cell Struct. Funct.* **33**, 61-73.

Kitajima, S., Miki, T., Takegami, Y., Kido, Y., Noda, M., Hara, E., Shamma, A. and Takahashi, C. (2011). Reversion-inducing cysteine-rich protein with Kazal motifs interferes with epidermal growth factor receptor signaling. *Oncogene* **30**, 737-750.

Klose, R. J., Kallin, E. M. and Zhang, Y. (2006). JmjC-domain-containing protein and histone demethylation. *Nat. Rev. Genet.* **7**, 725-727.

Koivisto, A. M., Ala-Mello, S., Lemmelä, S., Komu, H. A., Rautio, J. and Järvelä, I. (2007). Screening of mutations in the PHF8 gene and identification of a novel mutation in a Finnish family with XLMR and cleft lip/cleft palate. *Clin. Genet.* **72**, 145-149.

Krogan, N. J., Kim, M., Tong, A., Golshani, A., Cagney, G., Canadien, V., Richards, D. P., Beattie, B. K., Emili, A., Boone, C. et al. (2003). Methylation of histone H3 by Set2 in Saccharomyces cerevisiae is linked to transcriptional elongation by RNA polymerase II. *Mol. Cell. Biol.* **23**, 4207-4218.

Lagger, G., O'Carroll, D., Rembold, M., Khier, H., Tischler, J., Weitzer, G., Schuettengruber, B., Hauser, C., Brunmeir, R., Jenuwein, T. et al. (2002). Essential function of histone deacetylase 1 in proliferation control and CDK inhibitor repression. *EMBO J.* **21**, 2672-2681.

Laumonnier, F., Holbert, S., Ronce, N., Faravelli, F., Lenzner, S., Schwartz, C. E., Lespinasse, J., Van Esch, H., Lacombe, D., Goizet, C. et al. (2005). Mutations in PHF8 are associated with X linked mental retardation and cleft lip/cleft palate. *J. Med. Genet.* **42**, 780-786.

Li, B., Carey, M. and Workman, J. L. (2007). The role of chromatin during transcription. *Cell* **128**, 707-719.

Liu, G., Bollig-Fischer, A., Kreike, B., van de Vijver, M. J., Abrams, J., Ethier, S. P. and Yang, Z. Q. (2009). Genomic amplification and oncogenic properties of the GASC1 histone demethylase gene in breast cancer. *Oncogene* **28**, 4491-4500.

Liu, P., Jenkins, N. A. and Copeland, N. G. (2003). A highly efficient recombineering-based method for generating conditional knockout mutations. *Genome Res.* **13**, 476-484.

Lu, P. J., Sundquist, K., Baeckstrom, D., Poulsom, R., Hanby, A., Meier-Ewert, S., Jones, T., Mitchell, M., Pitha-Rowe, P., Freemont, P. et al. (1999). A novel gene (PLU-1) containing highly conserved putative DNA/chromatin binding motifs is specifically up-regulated in breast cancer. *J. Biol. Chem.* **274**, 15633-15645.

Martin, C. and Zhang, Y. (2005). The diverse functions of histone lysine methylation. *Nat. Rev. Mol. Cell Biol.* **6**, 8365-8370.

Migliorini, D., Lazzerini Denchi, E., Danovi, D., Jochemsen, A., Capillo, M., Gobbi, A., Helin, K., Pelicci, P. G. and Marine, J. C. (2002). Mdm4 (Mdmx) regulates p53-induced growth arrest and neuronal cell death during early embryonic mouse development. *Mol. Cell. Biol.* **22**, 5527-5538.

Mosammaparast, N. and Shi, Y. (2011). Reversal of histone methylation: biochemical and molecular mechanisms of histone demethylases. *Annu. Rev. Biochem.* **79**, 155-179.

Nagy, A., Gertsenstein, M., Vintersten, K. and Behringer, R. (2003). *Manipulating the Mouse Embryo: A Laboratory Manual*, 3rd edition, pp. 371-373. Cold Spring Harbor, NY: Cold Spring Harbor Laboratory Press.

Northcott, P. A., Nakahara, Y., Wu, X., Feuk. L., Ellison, D. W., Croul, S., Mack, S., Kongkham, P. N., Peacock, J., Dubuc, A. et al. (2009). Multiple recurrent genetic events converge on control of histone lysine methylation in medulloblastoma. *Nat. Genet.* **41**, 465-472.

Pedersen, M. T. and Helin, K. (2010). Histone demethylases in development and disease. *Trends Cell Biol.* **20**, 662-671.

Rantakari, P., Nikkilä, J., Jokela, H., Ola, R., Pylkäs, K., Lagerbohm, H., Sainio, K., Poutanen, M. and Winqvist, R. (2010). Inactivation of *Palb2* gene leads to mesoderm differentiation defect and early embryonic lethality in mice. *Hum. Mol. Genet.* **19**, 3021-3029.

Ruland, J., Sirard, C., Elia, A., MacPherson, D., Wakeham, A., Li, L., de la Pompa, J. L., Cohen, S. N., Mak, T. W. (2001). p53 accumulation, defective cell proliferation, and early embryonic lethality in mice lacking *tsg101*. *Proc. Natl. Acad. Sci. USA* **98**, 1859-1864.

Schaft, D., Roguev, A., Kotovic, K. M., Shevchenko, A., Sarov, M., Shevchenko, A., Neugebauer, K. M. and Stewart, A. F. (2003). The histone 3 lysine 36 methyltransferase, SET2, is involved in transcriptional elongation. *Nucleic Acids Res.* **31**, 2475-2482.

Steinman, H. A., Sluss, H. K., Sands, A. T., Pihan, G. and Jones, S. N. (2004). Absence of p21 partially rescues Mdm4 loss and uncovers an antiproliferative effect of Mdm4 on cell growth. *Oncogene* **23**, 303-306.

Suzuki, A., de la Pompa, J. L., Hakem, R., Elia, A., Yoshida, R., Mo, R., Nishina, H., Chuang, T., Wakeham, A., Itie, A. et al. (1997). *Brca2* is required for embryonic cellular proliferation in the mouse. *Genes Dev.* **11**, 1242-1252.

Tateishi, K., Okada, Y., Kallin, E. M. and Zhang, Y. (2009). Role of Jhdm2a in regulating metabolic gene expression and obesity resistance. *Nature* **458**, 757-761.

Terashima, M., Ishimura, A., Yoshida, M., Suzuki, Y., Sugano, S. and Suzuki, T. (2010). The tumor suppressor Rb and its related Rbl2 genes are regulated by Utx histone demethylase. *Biochem. Biophys. Res. Commun.* **399**, 238-244.

van Haaften, G., Dalgliesh, G. L., Davies, H., Chen, L., Bignell, G., Greenman, C., Edkins, S., Hardy, C., O'Meara, S., Teague, J. et al. (2009). Somatic mutations of the histone H3K27 demethylase gene *UTX* in human cancer. *Nat. Genet.* **41**, 521-523.

Wood, A. and Shilatifard, A. (2006). Transcriptional blackjack with p21. *Genes Dev.* **20**, 643-647.

Xiang, Y., Zhu, Z., Han, G., Ye, X., Xu, B., Peng, Z., Ma, Y., Yu, Y., Lin, H., Chen, A. et al. (2007). JARID1B is a histone H3 lysine 4 demethylase up-regulated in prostate cancer. *Proc. Natl. Acad. Sci. USA* **104**, 19226-19231.

Yamaguchi, T. P., Dumont, D. J., Conlon, R. A., Breitman, M. L. and Rossant, J. (1993). *flk-1*, an flt-related receptor tyrosine kinase is an early marker for endothelial cell precursors. *Development* **118**, 489-498.

Yang, Z. Q., Imoto, I., Fukuda, Y., Pimkhaokham, A., Shimada, Y., Imamura, M., Sugano, S., Nakamura, Y. and Inazawa, J. (2000). Identification of a novel gene, *GASC1*, within an amplicon at 9p23-24 frequently detected in esophageal cancer cell lines. *Cancer Res.* **60**, 4735-4739.

Yoshida, M., Ishimura, A., Terashima, M., Enkhbaatar, Z., Nozaki, N., Satou, K. and Suzuki, T. (2011). PLU1 histone demethylase decreases the expression of KAT5 and enhances the invasive activity of the cells. *Biochem. J.* **437**, 555-564.